PAPER

Check for updates

Copper-exchanged large-port and small-port mordenite (MOR) for methane-to-methanol conversion†

Amy J. Knorpp, [a] Ana B. Pinar,[b] Mark A. Newton, [a] Teng Li, [a] Adelaide Calbry-Muzyka [c] and Jeroen A. van Bokhoven [*ab]

Zeolite mordenite (MOR) is one of the most studied zeolites for the stepwise direct conversion of methane to methanol, but it also can exist in two forms: large port and small port. Here we report that the synthesis and selection of the parent mordenite is critical for optimizing productivity, and that large-port mordenite outperforms small-port mordenite for the stepwise conversion of methane to methanol.

Introduction

With over 200 different zeolite frameworks having been identified,[1] zeolites have found application in a multitude of chemical conversion processes. One such conversion is the direct partial oxidation of methane to methanol which has received recent attention as a potential way to use methane from small and dispersed sources worldwide.[2–4]

In this process, methane is directly converted to methanol through a stepwise[2] or catalytic procedure[5] where the zeolite acts as a support and provides a specific confined environment for the cation-exchanged copper to act as the site for the conversion. Several copper-exchanged zeolite frameworks have been shown to be active for this conversion, including mordenite (MOR),[2,5–9] ZSM-5 (MFI),[2,10] ferrierite (FER),[11] erionite (ERI),[12] offretite (OFF),[13] omega (MAZ),[14,15] and SSZ-13 (CHA).[16] Mordenite is the most widely studied zeolite framework with past studies identifying the active sites[8,17–20] and increasing productivity.[8,21] However despite these scientific efforts, the productivity of these materials is not sufficient for commercial interest;[22] therefore, a better understanding of what parameters affect the performance are needed.

Despite much of the work on mordenite and most other zeolites in this field, the parent zeolite itself and its synthesis is often overlooked as an opportunity for understanding and optimizing the conversion of methane to methanol. In the case of the direct conversion of methane to methanol, commercially

available mordenite is often used[2,5–9,20] instead of synthesizing in-house, because zeolite synthesis itself can be a time consuming task and can be laced with nuances.[23,24] In general when a zeolite is commercially available, it can be attractive to use, especially when multiple aspects of a conversion process need to be optimized.

Recently we showed for a non-commercially available zeolite, zeolite omega (MAZ), how slight changes in the zeolite synthesis and the parent zeolite can result in large differences in the methanol yield,[25] thus highlighting that the zeolite synthesis is an opportunity to further optimize this process. Additionally, we showed that the zeolite synthesis literature is an invaluable resource to uncover which unique nuances exist for each zeolite and how to harness them for optimizing a conversion process.

Mordenite synthesis has its own unique history with an era of intense research on two forms of mordenite: large-port and small-port.[26] Mordenite has a 12-ring channel (7.0 × 6.5 Å) with parallel 8-ring channels (5.7 × 2.6 Å); additionally there are 8-ring side channels (3.4 × 4.8 Å) that run perpendicular and interconnect the 12-ring and 8-ring channels.[1] Prior to the ability to specify the zeolite's structure through refinement of X-ray diffraction (XRD) data, adsorption studies of differently sized molecules were used instead to infer the pore structure. In the case of mordenite, early adsorption studies revealed that some synthesized mordenites did not adsorb molecules over 4 Å while others did.[26] This observation became even more puzzling when refinement of XRD data was able to conclude that large 12-ring channels are present in MOR, and that these should be able to accommodate such molecules.[26–28] This led to the distinction between large-port and small-port mordenite—specifically, large-port is identified as a mordenite that adsorbs >5 wt% of benzene (or a similarly sized molecule), while small-port typically adsorbs <5 wt% of the same molecule. However, this binary distinction is somewhat artificial as in reality there exists a continuum of port sizes. In fact, many syntheses for mordenite in the 1980–1990s were labelled large-port and small-

[a]*Institute for Chemical and Bioengineering, ETH Zurich, Vladimir-Prelog-Weg 1, Zurich 8093, Switzerland. E-mail: Jeroen.vanbokhoven@chem.ethz*

[b]*Laboratory for Catalysis and Sustainable Chemistry, Paul Scherrer Institute, Villigen 5232, Switzerland*

[c]*Bioenergy and Catalysis Laboratory, Paul Scherrer Institut, PSI, Villigen 5232, Switzerland*

† Electronic supplementary information (ESI) available. See DOI: 10.1039/d1ra04643h

port,[29–31] but today this practice has become less common. Furthermore, commercially available mordenite is not labelled as large- or small-port either, and the common surface area measurement (BET) cannot distinguish between these two possibilities. Since the practice of labelling large-port and small-port mordenite has become rare, the implications that these two forms may have for newly explored conversion processes, such as the direct conversion of methane to methanol, are entirely unknown. In this study we try to rectify this by examining a series of parent mordenites with different sized port forms and correlate them to their methanol yields in the stepwise conversion of methane to methanol.

Experimental

Zeolite synthetic procedure

Both commercial samples and in-house synthesized samples were selected for this study, and the silicon : aluminium ratio ranged from 6.5 to 15. Three mordenite are commercially available, and all have also been studied by various research groups for the conversion of methane to methanol.[6,32,33] They are also from three different zeolite suppliers (TOSOH, Zeolyst, and ZeoChem). An additional three mordenite samples were synthesized in-house by a hydrothermal synthesis technique but from three different synthesis formulations found in literature.[29,34,35]

In-house syntheses were conducted according to Jongkind et al. for MORSyn1,[34] Chi et al.[29] for MORSyn2, and Hincapie et al. for MORsyn3.[35] For MORSyn1, a slurry was prepared by initially mixing NaOH pellets (Sigma Aldrich, >97%) with deionized water. Fumed silica (Sigma Aldrich, 99%) and hexamethyleneimine (Sigma Aldrich, 99%) were then added slowly. Finally aluminium sulfate octahydrate (Sigma Aldrich, >98%) was added last. The final molar slurry composition was SiO_2 : AlO_3 : Na_2O : template : water = 30 : 15 : 7.3 : 11.4 : 636. Crystallization was conducted for 4 days at 170 °C. For MORSyn2, a slurry was prepared by initially mixing NaOH pellets (Sigma Aldrich, >97%) and KOH (Sigma Aldrich, 90%) with deionized water. Colloidal silica (Ludox, 30%) and aluminium hydroxide (Sigma Aldrich, reagent grade) were then added slowly. The final molar slurry composition was SiO_2 : AlO_3 : Na_2O : K_2O : water = 15.6 : 2 : 0.16 : 2.6 : 130. Crystallization was conducted for 4 days at 180 °C. Finally MORSyn3 was prepared by initially mixing NaOH pellets (Sigma Aldrich, >97%) with deionized water. Sodium aluminate (Strem Chemical, 99%) and then silica gel (Fisher, <200 mesh) were then added. Finally mordenite seeds (HZS-620NAA from TOSOH) were added the slurry (0.1 g of seed per 14 g of slurry). Crystallization was conducted for 1 day at 170 °C. All syntheses were carried out in a similar Teflon lined stainless steel autoclave with a capacity of 100 ml. The contents of the autoclave were filtered, rinsed with ethanol and water, and then dried at 333 K. The dried powder was then calcined at 550 °C for 8 hours with a ramp rate of 1 °C min^{-1}.

For methane to methanol conversion studies, each zeolite was stirred in 2 M solution of ammonium nitrate for 24 h at room temperature. The sample was filtered, rinsed, and dried.

The zeolite was then cation-exchanged with 0.0025 M of aqueous copper nitrate solution with 1 gram of material to 100 ml of aqueous solution. Each sample was exchanged three times. Between each exchange, a new solution was prepared, and the sample filtered, but not dried between exchanges.

Results and discussion

Adsorption studies

To determine if the mordenite was large-port or small-port, toluene adsorption of each sample was quantified by toluene adsorption breakthrough studies through a flow reactor that demonstrated to yield a high degree of isothermality.[36] First, each sample was sieved to a narrow 105–125 μm fraction, and 20 mg of the sieved sample was then placed between quartz wool in a 2 mm diameter borosilicate capillary. Initially each sample was dehydrated in situ at 450 °C for 1 h (ramp rate of 10 °C min^{-1}) in helium (10 ml min^{-1}) to remove any moisture filling the pores. The temperature was then lowered to 40 °C, and the gas was switched to bubbling helium (10 ml min^{-1}) through a bubbler filled with toluene which sat in an ice bath (2 °C). Toluene breakthrough was monitored by mass spectroscopy (m/z 91), and the quantity of toluene adsorbed was quantified by integration of the signal from the gas switch to the breakthrough completion. The calculations for the breakthrough experiment can be found in the ESI.† For each sample, the experiment was conducted twice. Table 1 shows the averaged results for the toluene adsorption study as well as basic information regarding each mordenite sample.

The toluene adsorption studies showed that two of the selected mordenites (MORComm1 and MORSyn3) had toluene adsorption over 6% wt, and thus the largest ports in the series. After these two samples, in decreasing order of toluene adsorption and thus of port size, follow MORComm3, MORComm2, MORSyn1, and MORSyn2.

Reaction studies

The selected mordenites were also tested in the stepwise conversion of methane to methanol. Each sample was cation exchanged with copper, and the copper loading for each samples is found in Table 1. The stepwise procedure for conversion of methane to methanol was as followed: (i) high temperature activation (ramp rate of 10 °C min^{-1}) in oxygen for 1 h at 450 °C (ii) purge (200 °C) in helium for 10 minutes (iii) reaction (200 °C) in methane (1 bar) for 30 minutes. After the reaction step, the reactor was cooled to room temperature in helium. The methanol was then extracted offline in 2 ml of deionized water and quantified by using gas chromatography. The methanol yield for each mordenite sample is shown in Table 1. The methanol yield was calculated on zeolite mass basis (dry) as well as on a copper molar basis.

The highest performing zeolites were MORComm1 and MorSyn3, both of which are large-port mordenite. By plotting the methanol yield against the toluene adsorption as shown in Fig. 1, there appears to be a benefit to a large-port mordenite. The difference between the shape of the two plots may be

Table 1 Summary of characteristics of mordenite samples tested for toluene adsorption and methane-to-methanol conversion

Name	Synthesis or supplier information	Si/Al ratio	BET surface area number [m² g⁻¹]	Cu loading [% wt Cu]	Methanol yield [μmol-MeOH/gram-zeolite]	Methanol yield [μmol MeOH/ μmol Cu]	Port determination	Toluene adsorption [% wt]
Commercially available mordenite								
MORComm1	CBV10ADS Zeolyst	6.5	425	3.4	89	0.16	Large port	6.6 ± 0.5
MORComm3	ZeoFlair800 Zeochem	10	410	4.5	60	0.08	Small port	3.7 ± 0.2
MORComm2	TOSOH HSZ-620HOA	7.5	400	3	58	0.12	Medium port	4.8 ± 0.3
In-house synthesized								
MORSyn1	Synthesis based on ref. 34	15	366	3.8	42	0.07	Small port	3.3 ± 0.2
MORSyn2	Synthesis based on ref. 29	10.6	379	2.4	20	0.05	Small port	2.0 ± 0.5
MORSyn3	Synthesis based on ref. 35	13.4	377	2	104	0.32	Large port	6.7 ± 0.3

explained by the often nonlinear relationship of the Cu loading and methanol yield, where at higher copper loadings the methanol yield often plateaus.[8,37] Both plots are provided for clarity.

A similar trend is also observed in literature for the three commercially available mordenites. Considering reported yields for the three commercial mordenites in literature, MORComm1 (CBV10ADS) has the highest reported methanol yields with >0.3 mol-methanol/mol-Cu being reported across several research groups.[32,37] For MorComm2 and MorComm3, the highest reported methanol yields in literature for each are low with methanol yields of <0.1 mol-methanol/mol-Cu,[6,14,21] thus following a similar trend to our study.

This distinction between large-port and small-port mordenite therefore appears more important than the Si/Al ratio, as both high methanol yielding mordenites included a range of Si/Al ratios. Similarly, the low performing small-port mordenites also included a range of Si/Al ratios. Additionally, selectivity does not appear to be affected by the large-port or small-port forms. MorComm1 and MorSyn1 were included in a previous study that focused on the Cu(II)/Cu(I) conversion with respect to selectivity. Both exhibited similar selectivities for methane-to-methanol conversion with Cu(I)/methanol ratio of ~2.6–2.7.[38]

It is pertinent to wonder what leads to large-port and small-port mordenite, but this has yet to be resolved despite many studies.[26,30,39,40] Several hypotheses have been proposed to explain this difference: pore blockage by (i) amorphous material (ii) inorganic cations, and (iii) the presence of fault domains. All of these could affect the methane-to-methanol conversion process by blocking active sites, by blocking the path for methanol extraction, or by altering the confined environment provided by the zeolite. Here we do not resolve why large-port and small-port mordenite exist, but we show that there are some striking implications that these forms have for the direct conversion of methane to methanol.

Conclusions

Several important conclusions can be made from this relatively simple study.

Firstly, toluene adsorption is a simple screening tool to select high methanol yielding mordenites.

Secondly, revisiting the concept of large-port and small-port forms may be important for other conversion processes, and also revisiting the reason behind the formation of these two
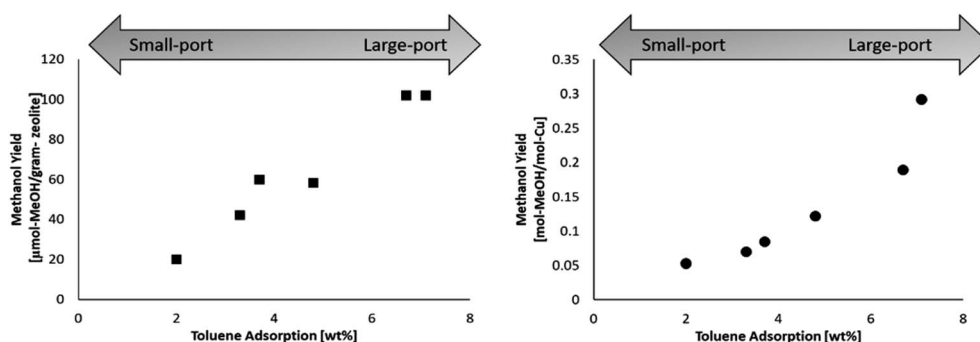

Fig. 1 (Left) Methanol yield per gram-zeolite in relation to the toluene adsorption. (Right) Methanol yield per mole copper in relation to the toluene adsorption.

forms could provide keys to develop additionally optimized materials.

Finally, the selection of the parent zeolite is critical to obtaining maximal the methanol yields. Optimization of the parent zeolite needs to be incorporated early, and early synthesis literature can provide invaluable information for this optimization.

Conflicts of interest

There are no conflicts to declare.

Notes and references

1 C. Baerlocher and L. B. McCusker, *Database of Zeolite Structures*, 2021, https://www.iza-structure.org/databases/.

2 M. H. Groothaert, P. J. Smeets, B. F. Sels, P. A. Jacobs and R. A. Schoonheydt, *J. Am. Chem. Soc.*, 2005, **127**, 1394–1395.

3 R. Horn and R. Schlögl, *Catal. Lett.*, 2015, **145**, 23–39.

4 J.-P. Lange, V. L. Sushkevich, A. J. Knorpp and J. A. van Bokhoven, *Ind. Eng. Chem. Res.*, 2019, **58**, 8674–8680.

5 K. Narsimhan, K. Iyoki, K. Dinh and Y. Román-Leshkov, *ACS Cent. Sci.*, 2016, **2**, 424–429.

6 E. M. Alayon, M. Nachtegaal, M. Ranocchiari and J. A. van Bokhoven, *Chem. Commun.*, 2012, **48**, 404–406.

7 P. Vanelderen, J. Vancauwenbergh, M. L. Tsai, R. G. Hadt, E. I. Solomon, R. A. Schoonheydt and B. F. Sels, *ChemPhysChem*, 2014, **15**, 91–99.

8 S. Grundner, M. A. C. Markovits, G. Li, M. Tromp, E. A. Pidko, E. J. M. Hensen, A. Jentys, M. Sanchez-Sanchez and J. A. Lercher, *Nat. Commun.*, 2015, **6**, 7546.

9 V. L. Sushkevich, D. Palagin, M. Ranocchiari and J. A. van Bokhoven, *Science*, 2017, **356**, 523–527.

10 N. V. Beznis, B. M. Weckhuysen and J. H. Bitter, *Catal. Lett.*, 2010, **138**, 14–22.

11 D. Pappas, E. Borfecchia, M. Dyballa, K. A. Lomachenko, A. Martini, G. Berlier, B. Arstad, C. Lamberti, S. Bordiga, U. Olsbye, S. Svelle and P. Beato, *ChemCatChem*, 2019, **11**, 621–627.

12 J. Zhu, V. L. Sushkevich, A. J. Knorpp, M. A. Newton, S. C. M. Mizuno, T. Wakihara, T. Okubo, Z. Liu and J. A. Van Bokhoven, *Chem. Mater.*, 2020, **32**, 1448–1453.

13 A. J. Knorpp, M. A. Newton, S. C. M. Mizuno, J. Zhu, H. Mebrate, A. B. Pinar and J. A. Van Bokhoven, *Chem. Commun.*, 2019, **55**, 11794–11797.

14 M. B. Park, S. H. Ahn, A. Mansouri, M. Ranocchiari and J. A. van Bokhoven, *ChemCatChem*, 2017, **9**, 3705–3713.

15 A. J. Knorpp, A. B. Pinar, M. Newton, V. Sushkevich and J. A. van Bokhoven, *ChemCatChem*, 2018, **10**, 5593–5596.

16 M. J. Wulfers, S. Teketel, B. Ipek and R. F. Lobo, *Chem. Commun.*, 2015, **51**, 4447–4450.

17 P. Vanelderen, B. E. R. Snyder, M. L. Tsai, R. G. Hadt, J. Vancauwenbergh, O. Coussens, R. A. Schoonheydt, B. F. Sels and E. I. Solomon, *J. Am. Chem. Soc.*, 2015, **137**, 6383–6392.

18 E. M. C. Alayon, M. Nachtegaal, A. Bodi, M. Ranocchiari and J. A. van Bokhoven, *Phys. Chem. Chem. Phys.*, 2015, **17**, 7681–7693.

19 V. L. Sushkevich, D. Palagin and J. A. van Bokhoven, *Angew. Chem., Int. Ed.*, 2018, **57**, 8906–8910.

20 G. Brezicki, J. D. Kammert, T. B. Gunnoe, C. Paolucci and R. J. Davis, *ACS Catal.*, 2019, **9**, 5308–5319.

21 P. Tomkins, A. Mansouri, S. E. Bozbag, F. Krumeich, M. B. Park, E. M. C. Alayon, M. Ranocchiari and J. A. van Bokhoven, *Angew. Chem., Int. Ed.*, 2016, **55**, 5557–5561.

22 Z. R. Jovanovic, J.-P. Lange, M. Ravi, A. J. Knorpp, V. L. Sushkevich, M. A. Newton, D. Palagin and J. A. van Bokhoven, *J. Catal.*, 2020, **385**, 238–245.

23 M. E. Davis and R. F. Lobo, *Chem. Mater.*, 1992, **4**, 756–768.

24 J. Cejka, H. V. Bekkum, A. Corma and F. Schueth, in *Introduction to Zeolite Science and Practice*, Elsevier Science, Amsterdam, 3rd edn., 2007.

25 A. J. Knorpp, M. A. Newton, V. L. Sushkevich, P. P. Zimmermann, A. B. Pinar and J. A. van Bokhoven, *Catal. Sci. Technol.*, 2019, **9**, 2806–2811.

26 L. Sand, in *Molecular Sieves*, 1968, p. 71.

27 R. M. Barrer and D. L. Peterson, *Proc. R. Soc. London, Ser. A*, 1964, 466–485.

28 W. M. Meier, *Z. Kristallogr.*, 1961, 439–450.

29 C. H. Chi and L. B. Sand, *Zeolites*, 1985, **5**, 309–312.

30 F. Raatz, C. Marcilly and E. Freund, *Zeolites*, 1985, **5**, 329–333.

31 A. A. Shaikh, P. N. Joshi, N. E. Jacob and V. P. Shiralkar, *Zeolites*, 1993, **13**, 511–517.

32 D. K. Pappas, A. Martini, M. Dyballa, K. Kvande, S. Teketel, K. A. Lomachenko, R. Baran, P. Glatzel, B. Arstad, G. Berlier, C. Lamberti, S. Bordiga, U. Olsbye, S. Svelle, P. Beato and E. Borfecchia, *J. Am. Chem. Soc.*, 2018, **140**, 15270–15278.

33 Y. R. Jeong, H. Jung, J. Kang, J. W. Han and E. D. Park, *ACS Catal.*, 2021, 1065–1070.

34 H. Jongkind, K. P. Datema, S. Nabuurs, A. Seive and W. H. J. Stork, *Microporous Mater.*, 1997, **10**, 149–161.

35 B. O. Hincapie, L. J. Garces, Q. Zhang, A. Sacco and S. L. Suib, *Microporous Mesoporous Mater.*, 2004, **67**, 19–26.

36 M. A. Newton, S. Checchia, A. J. Knorpp, D. Stoian, W. Van Beek, H. Emerich, A. Longo and J. A. Van Bokhoven, *Catal. Sci. Technol.*, 2019, **9**, 3081–3089.

37 S. C. M. Mizuno, S. Dulnee, T. C. P. Pereira, R. J. Passini, E. A. Urquieta-gonzalez, J. M. R. Gallo, J. B. O. Santos and J. M. C. Bueno, DOI: DOI: 10.1016/j.cattod.2020.11.027.

38 M. A. Newton, A. J. Knorpp, A. B. Pinar, V. L. Sushkevich, D. Palagin and J. A. Van Bokhoven, *J. Am. Chem. Soc.*, 2018, **140**, 10090–10093.

39 F. Raatz, E. Freund and C. Marcilly, *J. Chem. Soc., Faraday Trans.*, 1983, **79**, 2299–2309.

40 P. C. Van Geem, K. F. M. G. J. Scholle and G. P. M. Van Der Velden, *J. Phys. Chem.*, 1988, **92**, 1585–1589.